Electrodegradation of phenol using pure and nanocomposite cerium oxides

M. El Hajji[1], A. Hallaoui[1], L. Bazzi[1*], O. Jbara[2], A. Benlhachemi[1], M. Hilali[1], A. Tara[2], B. Bakiz[1,3]

[1] *Material and Environment Laboratory (LME), Faculty of Sciences, Agadir, Morocco*
[2] *Engineering and Materials Science Laboratory (LISM), UFR Sciences, University of Reims, France*
[3]*Microelectronic Materials and Nanosciences Institute of Provence, CNRS UMR 7334, South Toulon-Var University, France*

Abstract

This paper presents an application of electrodeposited ceria "CeO$_2$" and "CeO$_2$-CaO" nanocomposite oxides thin films to electrochemical degradation of phenol known as organic pollutant. The experimental techniques used were the chronopotentiometry, the chemical oxygen demand and the UV-Visible spectroscopy. A comparative study of electrocatalytic effectiveness of as-electrodeposited thin films and the Boron doped diamond electrodes was made. The effect of using different supporting electrolytes "NaCl, KCl, Na$_2$CO$_3$, H$_2$SO$_4$ and Na$_2$SO$_4$" during the galvanostatic electrolysis of phenol was investigated. It was observed that the chemical oxygen demand (COD) was only achieved at appreciable rate of degradation when NaCl was used as the supporting electrolyte. The achieved mineralization percentage of phenol was about 33%, 58%, and 72% on pure ceria «SS/CeO$_2$», on nanocomposite ceria «SS/CeO$_2$-CaO» and on Boron doped diamond electrodes respectively. Compared with SS/CeO$_2$, the SS/CeO$_2$-CaO anode has shown more performance and rapidity in the COD removal in the same electrolysis device.

Keywords: Electrodeposited ceria, CeO$_2$-CaO, Phenol, COD, BDD, electrocatalytic effectiveness

1. Introduction

Phenol is present in wastewater from the manufacture of phenolic resins, synthetic chemical plants, plastics, and some pesticides. Following its toxicity and difficulty to degrade, the presence of phenol becomes a considerable problem to environment and human health [1]. Various advanced oxidation processes, including photochemical reactions, supercritical water oxidation, and Fenton oxidation have been made to degrade and destroy this aromatic organic [2,3]. Electrochemical degradation is another alternative that has attracted considerable research attention [4-6]. It is able to treat aqueous charged organic matter solutions [7-10]. This method has attracted considerable research attention mainly on toxic organics which can be effectively oxidized to biodegradable products [4,11,12]. Electrochemical oxidation has the advantage of being able to react on the pollutants, especially by direct anodic oxidation. Moreover, the catalyst/electrode is immobilized (thus reducing the need to separate the catalyst from the reaction mixture), the variables (current and potential) are easily controlled and the cost of the equipment is generally not expensive [13]. This electrooxidation is based on the generation of a hydroxyl radical HO$^•$ being adsorbed on the surface of the electrode by oxidation of water on an electrode with great oxygen over pressure [14]. Indeed, the effectiveness of electrochemical oxidation treatment depends on the nature of the anodes that are used in the process [15-17]. Hence, the degradation pathway of aromatic organics on different anodes remains a subject for investigation.

Therefore, the aim of this work is then to study the electrochemical process for the degradation of phenol in aqueous solutions using different anodes. The process was studied under galvanostatic polarization mode in acidic media using BDD, SS/CeO$_2$ and SS/CeO$_2$-CaO as anodes. The degradation rate of the studied organic pollutant, the efficiency and the limits of such a technique were investigated according to experimental parameters such as the supporting electrolyte nature and the initial concentration of electrolyte.

2. Materials and methods

2.1. Materials

2.1.1 Chemicals

In this work, all solutions were freshly prepared in the laboratory and contain phenol with a concentration of 200 mg.L^{-1}. Double distilled water was used. NaCl, KCl, Na$_2$SO$_4$, Na$_2$CO$_3$, and H$_2$SO$_4$ were employed as conductive electrolytes.

2.1.2 BDD, SS/CeO$_2$ and SS/CeO$_2$-CaO electrodes

The Boron-doped diamond « BDD » is a new electrode. Recently, it has received great attention [18, 19]. The wide potential window and the high anodic stability of the BDD promote its applications in the electrochemical oxidation of organics [20, 21]. The BDD electrode was provided by CSEM Company. It was synthesized by the chemical vapor deposition technique (HF-CVD) [22]. For CeO$_2$ and CeO$_2$-CaO thin films preparation, a Stainless steel (SS) plate was used as support or substrate. The films were galvanostatically electrodeposited using a cathodic electrodeposition process. The detail of preparation method of SS/CeO$_2$ and SS/CeO$_2$-CaO anodes can be found in Refs [23].

2.1.3 Bulk electrolysis

The cyclic voltammetry (CV) spectra and the electrochemical measurements were performed using a computer controlled by Potentiostat/Galvanostat PGP 201 Radiometer Copenhagen Voltalab.TM associated to "Volta-Master 4" software. A conventional three electrodes cell (100 cm^3) thermoregulated glass cell was used. The anode was a square plate of BDD electrode with an effective surface area of 2 cm^2, or a disk plate of « SS/CaO-CeO$_2$ or SS/CeO$_2$ electrodes » with an effective surface area of 0.2 cm^2, whereas the cathode was a platinum electrode. The distance between the anode and the cathode was set at 1.5 cm. A saturated calomel electrode (SCE) was used as a reference. Thereafter, a comparative study was executed using these anodes. The cell was connected to a water bath in order to control and keep the temperature constant at 30°C. It was set on a magnetic stirrer for continuous mixing. The operating current density during degradation of phenol was 30mAcm^{-2}. The degradation took 240 to 300 minutes.

2.2 Methods
2.2.1 COD Analysis

The chemical oxygen demand "COD" measurement permitted the evaluation of the kinetic of organic matter rottenness. LOVIBOND Checkit COD VARIO device was used for all measures of COD. This test is useful for the characterization of all raw waters and the waters treated by physicochemical ways [24]. The samples were taken during electrolysis with various time intervals. The rate of mineralization was expressed as a percentage of COD. This rate was given for various reaction times by this relation:

$$\%COD= [(COD_i – COD_t)/ COD_i]*100$$

With:
- COD$_i$: value of COD (mg/L of O$_2$) at initial moment
- COD$_t$: value of COD (mg/L of O$_2$) at t moment

2.2.2 UV-Vis Measurements

The UV absorbency spectrogram at wavelength range 190-1100 nm was recorded using a TU1800-UV-vis spectrometer. The concentration of phenol was 200 mg/L with 2% NaOH. An UV detector was used with a wavelength setting at 270 nm.

3. Results and discussion
3.1. Effect of the supporting electrolyte

Prior each electrolysis, cyclic voltammetry investigations were performed in order to characterize the electrolyte used. Cyclic voltammetry is a useful technique for probing the processes that occur at the electrode/solution interface [25]. The current variation that results when the electrode potential is varied can provide valuable insight into the reactions that occur at the electrode surface. Figure 1 represents the voltammetric profiles of the different supporting electrolytes in a 2% NaCl, 2% KCl, 2% H$_2$SO$_4$, 2% Na$_2$SO$_4$, and 2% Na$_2$CO$_3$ solution with the presence of 200 mgL^{-1} of phenol.

In 2% NaCl, it can be observed that phenol promotes a significant increase in charge or current associated with the oxygen evolution reaction on the BDD electrode. The KCl response remains still close to NaCl response. However, the other supporting electrolyte response presents a considerable decrease in charge when phenol is added. Indeed, the NaCl were the most effective conductive electrolyte for the electrocatalytic degradation of the investigated phenol. These results would indicate that, the NaCl electrolyte becomes the dominant active substance [26-29], its presence is essential, and the phenol can decreased rapidly.

3.2 Effect of NaCl concentration

The investigation of NaCl concentration effect has been performed. Figure 2 shown the effect of the supporting electrolyte concentration on the degradation of phenol solution, carried out at 30 mA/cm^2. As shown in this Figure, the utilization of supporting electrolyte has the ability to reduce considerably the chemical oxygen demand (COD). The electrochemical degradation of the organic substrate is achieved at reasonable rate only in the presence of 2% NaCl concentration.
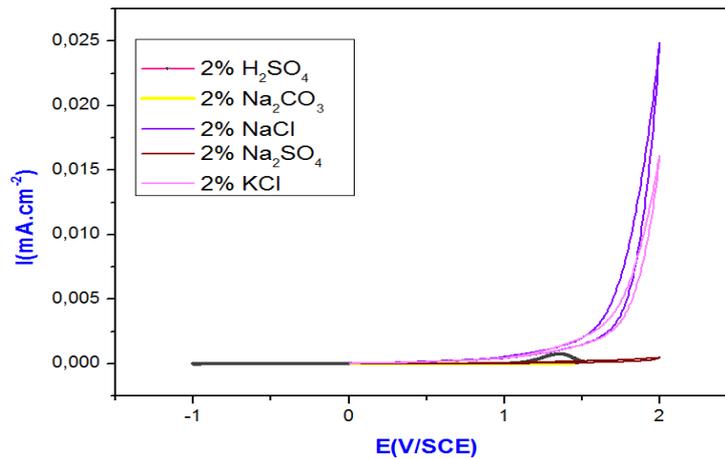
Figure 1. Voltammetric profiles of the BDD electrode in different supporting electrolytes of phenol 200 mg.L^{-1}. Auxiliary electrode: platinum; reference electrode: SCE; scan rate: 50 mVs^{-1}.
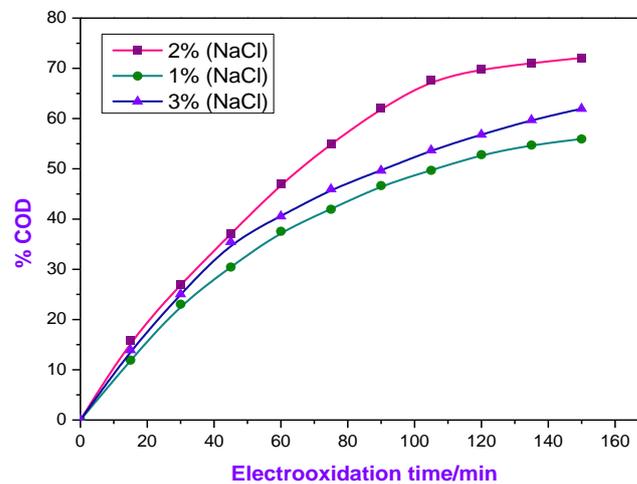
Figure 2. Effect of NaCl concentration on the % COD (200 mg.L^{-1} phenol solution, 30 mA.cm^{-2}, Working electrode: BDD; Auxiliary electrode: platinum; reference electrode: SCE, T = 30°C).

The achieved % COD values were 72%, 57 %, and 49% respectively for 2%, 3% and 1% NaCl. The mechanism of electrochemical mineralization can be direct; in this case there is an oxidation of phenol on the electrode using some mediators like HO$^{\bullet}$ radicals [30,31]. These radicals result from water molecule discharge as follow [27,32-34]:

$$H_2O \quad \rightarrow \quad HO^{\bullet} \; + \; H^+ \; + \; e^- \tag{1}$$

The oxidation rate of the reaction is calculated from the slope value of the plot of Ln[COD(0)/COD(t)] versus time (Figure.3). Indeed, the anodic oxidation kinetics of organic matter by the electrogenerated hydroxyl radicals HO$^{\bullet}$ is assumed to be a first-order kinetics and the hydroxyl radicals concentration is constant during electrolysis. According to the results in Figure 3, the straight lines obtained in these plots were in agreement with a pseudo first-order % COD removal, the COD values decreased almost exponentially. Increasing the supporting electrolyte concentration increases and facilitates the diffusion flux of organic matter towards the anode surface. However, when the supporting electrolyte exceeds a certain value of concentration (in this case over 2% NaCl), the % COD removal follows always pseudo first-order kinetics but a greater decrease of % COD is found. The apparent rate constant change with the supporting electrolyte concentration is given in Table 1. Several authors [35-39] also explained such a behaviour.

Hence, the using of NaCl electrolyte needs to be carefully optimized, considering the degradation efficiency, cost and relevant emission standards. It was more suitable for this study. Therefore, in the presence of a less concentration of chloride ions (2% NaCl) allows inhibiting the water discharge into oxygen, and promotes hydroxyl, chloride, and oxycloride radical's formation.

675
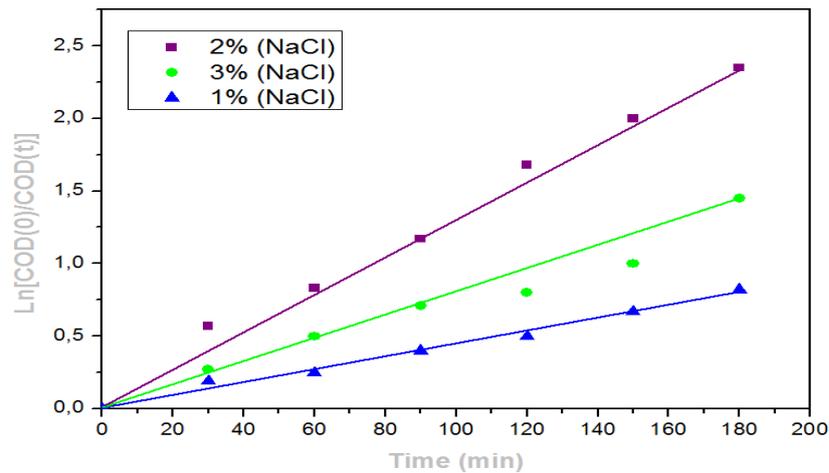
Figure 3. Linear regression for % COD removal with time during the electrochemical oxidation of phenol on the BDD anode for different supporting electrolyte concentrations at T = 30°C.

Table 1: Apparent rate constants of phenol removal fitted using a first order model for different NaCl concentrations

NaCl Concentration	$k \, (\times 10^{-3} \, min^{-1})$	R^2
1%	1.61	0.986
2%	2.66	0.993
3%	1.01	0.975

3.3 Effect of current density

The influence of the current density on the COD removal during the electrooxidation of phenol is shown in Figure 4. As expected, the COD abatement is faster as the current density is higher. Optimum current density is 30mAcm^{-2}, at which the maximum removal of phenol is observed. The results are a logical consequence of the major quantity of charge passing in solution. Hence, the application of the highest current density can be suggested in order to obtain the complete abatement of the organic content in the smallest time. Patently, the efficiency of the oxygen evolution reaction is larger at higher current densities.
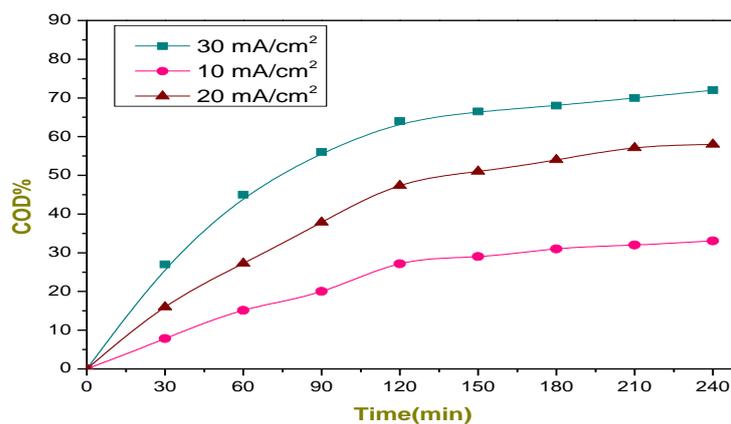
Figure 4. Influence of the applied current density on the % COD (200 mg.L^{-1} phenol solution, working electrode: BDD; Auxiliary electrode: platinum; reference electrode: SCE, T = 30°C).

After 240 min time of electrolysis, the COD percent removal increased from 33% to 73% when the current density increased from 10 to 30 mA.cm^{-2}. This behavior indicates that in these experimental conditions, the oxidation of phenol is completely under mass transport control and an increase of the applied current favors only the secondary reaction of oxygen evolution:

$$2H_2O \quad \rightarrow \quad O_2 \ + \ 4H^+ \ + \ 4e^- \tag{2}$$

3.4 Influence of anode composition on degradation rate of phenol

The first part of this work had allowed us to determine some optimal parameters. Now we focus on the electrocatalytic effectiveness comparison between BDD, SS/CeO_2 and SS/CeO_2-CaO anodes. The goal is to classify the anodes according to the best electrocatalytic efficiency respect to the electrochemical degradation of phenol.

3.4.1 Galvanostatic study

Figure 5 shows the evolution of potential with time during the electrodeposition process. Globally, there is a continuous decrease in potential with time, nevertheless different distinct steps are observed. At the early beginning application of current density, the potential increases drastically (0 to 2940 mV). Over the first 500 s, the current decreases, and reaches a plateau value of about 2853 mV. The potential decrease continues again towards the steady value of 2840 mV after 1200 s. For all three kinds of anode used, the shape of the curve was the same, only the oxidation potential was changed.
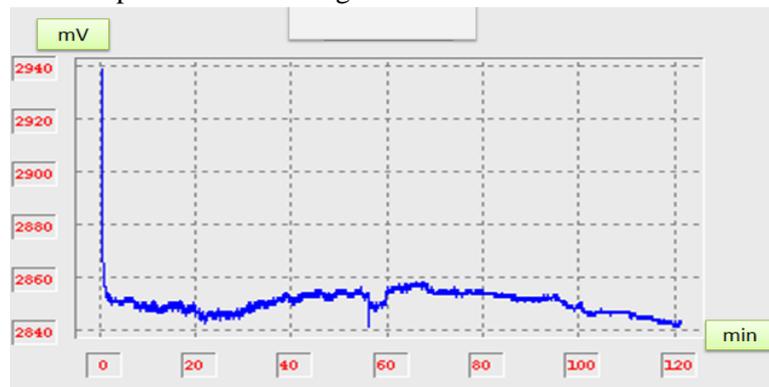
Fig. 5. Evolution of the potential with time during the electrochemical degradation of phenol on the SS/CeO_2-CaO anode

3.3.2 Variation of pH study

The pH of the solution was measured during the electrochemical degradation. It varies during the electrolysis process « Figure 6 » irrespective of the nature of the working electrode. On BDD anode, the pH values dropped first from the initial value of 5.7 with no sign of oxidation, after 90 min of degradation, the pH remained at around 4.4, while the phenol was being electrochemically oxidized. After some minutes, it began to increase and it approached to 7. On SS/CeO_2-CaO and SS/CeO_2 anodes, the pH remained at around 5.4 and 5.5, respectively. On SS/CeO_2-CaO anode; and after 60 minutes of degradation, the pH became more acid, this phenomenon was not observed for the degradation process on other electrodes. On SS/CeO_2, it decreases to a value of 4.3, and it increases slowly during the degradation. Indeed, on the three kinds of anode, the intermediates of degradation are different.
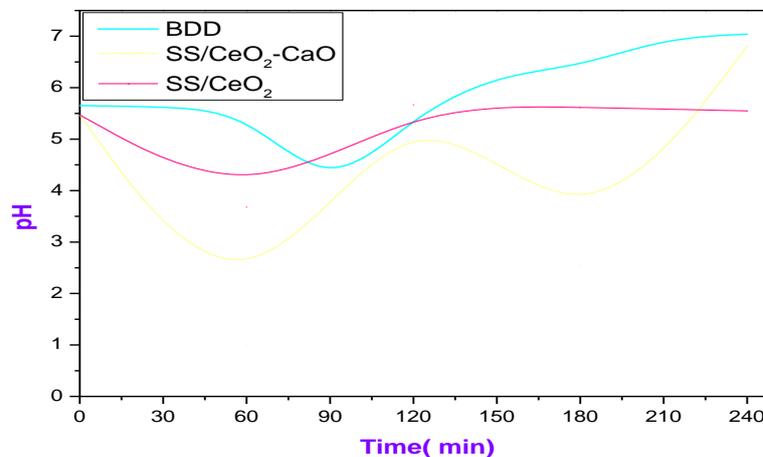
Figure 6. pH variation during electrochemical degradation of phenol on SS/CeO_2-CaO, SS/CeO_2 and BDD anodes.

3.3.3 Variation of the coloration during electrolysis

The phenol solutions exhibited color changes during the electrolysis process (Figure 7). Table 2 shows all color changes recorded. During electrolysis « on the BDD anode », the liquid turned to dark yellow in the first 20 minutes of phenol oxidation. The yellow color began to fade when the phenol concentration was reduced. Finally the color had almost disappeared after about 180 minutes (Table 2).

Table 2. Variation of the coloration during the degradation of phenol on the three kinds of anode.

Time (min)	Coloration variation /on BDD	Formulate Probable metabolite	Coloration variation /on SS/CeO$_2$	Formulate Probable metabolite	Coloration variation SS/CeO$_2$-CaO	Formulate Probable metabolite
0	colorless	C$_6$H$_5$OH	colorless	C$_6$H$_5$OH	colorless	C$_6$H$_5$OH
20	Dark yellow	Phenate	Yellow	phenate	Clear brown	Phenate
40	Clear brown	Benzoquinone	Dark yellow	Catechol	Brown	Hydroquinone
60	clear yellow	Aliphatic compound	yellow	Benzoquinone+ Catechol	yellow	Benzoquinone
180	colorless	Water	Clear yellow	Aliphatic acids	colorless	Aliphatic acids
240	colorless	Water	Very Clear yellow	Aliphatic acids + water	colorless	Water
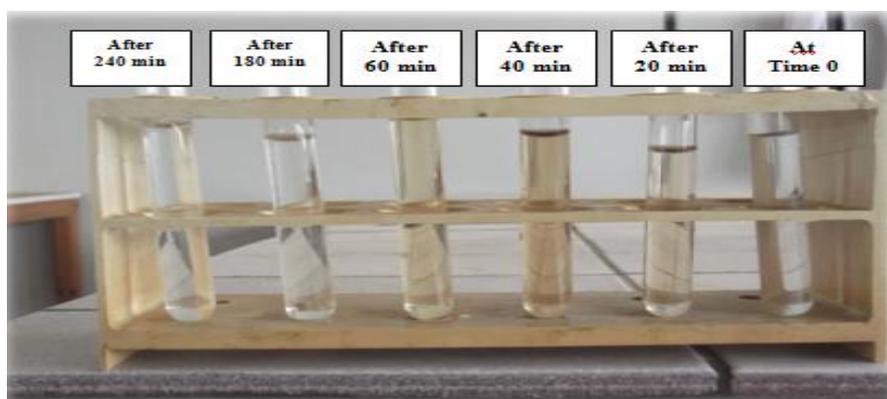
Figure 7. Color variation during the electrochemical degradation of phenol on SS/CeO$_2$-CaO anode

In previous works, the mechanism of electrocatalytic oxidation, in which phenol is degraded by the hydroxyl radical, has already been confirmed by many researchers [32,35,40-43]. On the SS/CeO$_2$-CaO anode, the solution became brown and turned to yellow. Generally, the yellow color is caused by Benzoquinone, which is produced during the phenol degradation. In degradation process, the phenol oxidizes to hydroquinone then into Benzoquinone. The concentration of these products in solution increased within the first 40 min and then rapidly decreases. The Benzoquinone and hydroquinone are almost disappeared after 120 min, due to the attack of free radicals on these compounds and resulting in ring opening reaction to form aliphatic organic acids. When phenol is degraded to aliphatic carboxylic acids the wastewater will become more biodegradable and less toxic. According to the variation of pH of the solution (Figure 6), it can be seen that, the concentration of aliphatic organic acids increases during the first 160 min and then begins to decrease rapidly. This decrease could be due to mineralization of formed organic acids to CO$_2$ and H$_2$O, allowing the increase of pH after 200 min of degradation. A comparison of reaction products formed by phenol oxidation on the all three kinds of anodes used in this study showed that the reaction products are different depending on the type of anode used. However, all reactions probably occur following the same mechanism, i.e. hydroxyl radical attack the phenol, which becomes phenate ion oxidized to hydroquinone then into Benzoquinone, or Catechol. Subsequent oxidation of these products, after opening of the aromatic ring, leads to the formation of aliphatic carboxylic acids, mineralized finally to CO$_2$ and H$_2$O when the anode is more efficient.

3.3.4 COD removal and UV-Visible absorbency measurement

Periodic analysis of % COD removal was carried out during electrolysis to determine the kinetics of degradation of phenol on the three above mentioned electrodes. Figure 8 shows the evolution of % COD according to the time of electrolysis and the nature of working electrode. On BDD, it became an important

percentage of degradation in the first time of electrolysis. However, this % COD remained relatively weak for the first 30 min on SS/CeO$_2$-CaO and SS/CeO$_2$ electrodes. At the end of electrolysis that occurs at 240 min, the % COD took the values of 33%, 58% and 71% respectively for the degradation of phenol on SS/CeO$_2$, SS/CeO$_2$-CaO, and BDD electrodes.

Figure 8 is UV-Visible absorbency spectrograms in the wavelength range 190–1100 nm carried out during electrolysis. The peaks of phenol at 270 nm decrease with prolonging electrolysis time, and the new peaks of metabolite (after 60 min of electrolysis) grow in the initial period, and then come down. This result was in agreement with % COD removal measurement.

The change of %COD exhibits an exponential behavior indicating a first order reaction kinetics for the electrooxidation reaction. Hence, the apparent observed pseudo first-order rate constant k_{app} can be determined by plotting the Ln(COD$_0$/COD$_t$) against time for different used anodes . The results are presented in Table 3.

The concentration of OH$^{\bullet}$ can be approximated in a steady state. The integrated oxidation rate expression can be written as follows:

$$Ln(COD_0/COD_t) = K_{app}t$$
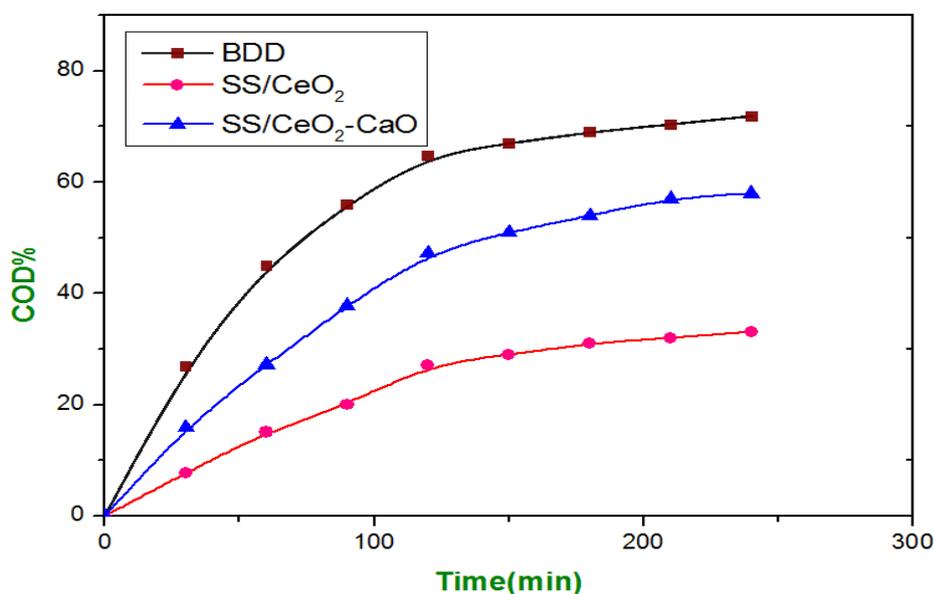
Figure 8. Electrochemical degradation of phenol onto SS/CeO$_2$-CaO, SS/CeO$_2$ and BDD anodes: % COD evolution

Table 3. Variation of the values of the rate constant and the %COD depending on the used anode

Anode	k ($\times 10^{-4}$ min^{-1})	COD removal (%)
BDD	33.31	72
SS/CeO$_2$	12.6	33
SS/CeO$_2$-CaO	27.01	58

From this result, the SS/CeO$_2$-CaO anode has shown more performance and rapidity in the COD removal in the same electrolysis device.

Figure 9 shows the UV-Visible absorbency spectrograms carried out during galvanostatic electrolysis in aqueous solution using SS/CeO$_2$-CaO anode. It can be observed that the absorption spectrum of phenol is characterized by a band in the UV region with its maxima located at 270 nm. The absorption of the maxima "270 nm" decreases with the time and almost disappears after about 60 min of degradation, accompanied by the appearance of a new band located at 310 nm referring to the apparition of Benzoquinone. The movement and appearance of this new band indicates the apparition of metabolite (after 60 min of electrolysis) witch grow in the initial period, and then come down. This result was in agreement with % COD removal measurement.
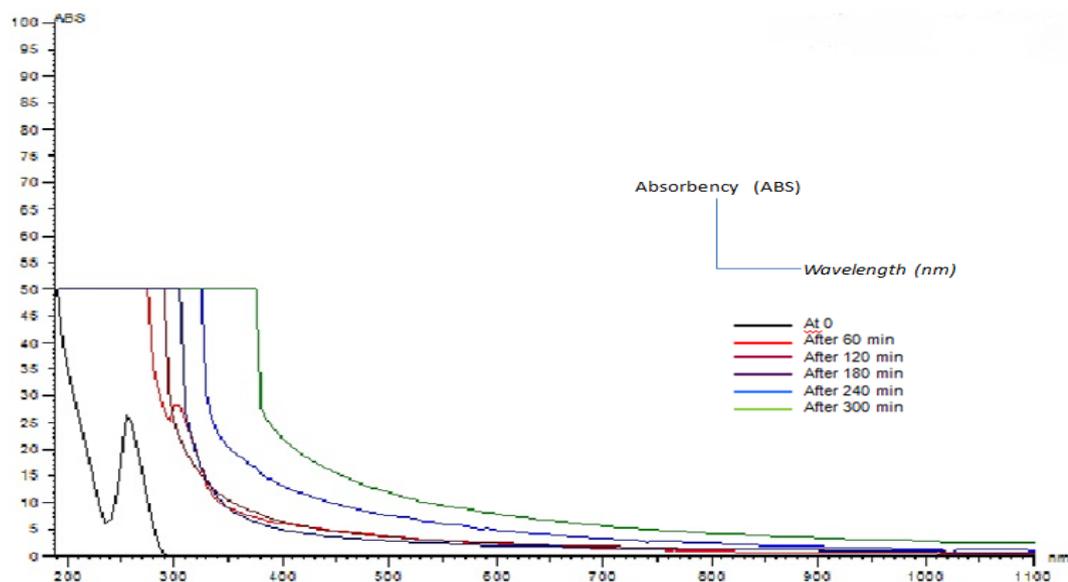
Figure 9. UV spectra of the phenol during the electrochemical degradation at some electrolysis time.

Conclusion

The electrochemical degradation of phenol has been investigated using three kinds of anodes such as SS/CeO$_2$-CaO, SS/CeO$_2$ and BDD electrodes. The experimental results showed that:

- The best results were obtained when electrolyses were carried out at high densities, 30 mAcm^{-2}, and in the presence of supporting electrolyte NaCl (2%), but decreases for higher values of supporting electrolyte, due to the improvement of this reaction.
- The extraordinary high activity of hydroxyl radicals from the water discharge and the removal of COD were well described by pseudo first-order kinetics.
- The best obtained conditions for COD removal on the BDD anode to degrade phenol solutions involve operating at 30 mAcm^{-2} and 30 $^{\circ}$C. This arrangement allows to completely degrading the organic matter in just 240 min.
- For comparison, the degradation of phenol on SS/CeO$_2$-CaO anode provided an oxidation rate and % COD removal higher than on SS/CeO$_2$ anode in the same operating conditions. This preliminary study suggests that anodic oxidation with CeO$_2$-CaO nanocomposite oxides electrode constitutes a viable method for the treatment effluents contaminated with phenol.

References

1. Luttrell W.E., *Chem Health Safe*. 10 (2003) 20.
2. Brillas E., Mur E., Sauleda R., Sanchez L., Peral J., Domenech X., Casado J., Aniline. *J Appl Catal B Environ*. 16 (1998) 31.
3. Esplugas S., Gimenez J., Contreras S., Pascual E., Rodriguez M., *Water Res*. 36 (2002) 1034.
4. Comninellis C., *Electrochimica Acta*. 39 (1994) 1857.
5. Rodgers J.D., Jedral W.J., Bunce N.J., *Environ Sci Technol*. 33 (1999) 1453.
6. Brillas E., Calpe J.C., Casado J., *Water Res*. 34 (2000) 2253.
7. Feng C.P., Sugiura N., Shimada S., Maekawa T., *J Hazard Mater B*. 103 (2003) 65.
8. Sanromán M.A., Pazos M., Ricart M.T., Cameselle C., *Electrochemical decolourisation of structurally different dyes, Chemosphere*. 57 (2004) 233.
9. Rajkumar D., Palanivelu K., *J Hazard Mater B*. 113 (2004) 123.
10. Quiroz M.A., Reyna S., Martínez C.A., Ferro S., De Battisti A., *Appl Catal B: Environ*. 59 (2005) 259.
11. Pulgarin C., Adler N., Péringer P., Comninellis Ch., *Water Res*. 28 (1994) 887.
12. Wabner D., Grambow C., *J Electroanal Chem*. 95 (1985) 195.

13. Juttner K., Galla U., Schmieder H., *Electrochim Acta*. 45 (2000) 2575.
14. Zaviska F., Drogui P., Mercier G., and Blais J.F., *Journal of Water Science*. 22 (2009) 535.
15. Feng Y.J., Li X.Y., *Water Res*. 37 (2003) 2399.
16. Stucki S., Kötz R., Carcer B., Suter W., *J Appl Electrochem*. 21 (1991) 99.
17. Chen G.H., *Electrochemical technologies in wastewater treatment. Sep Purif Technol*. 38 (2004) 11.
18. Pleskov Yu.V., *Russ Chem Rev*. 68 (1999) 381.
19. Swain G.M., Anderson A.B., Angus J.C., *Materials Research Society*. 23 (1998) 56.
20. Bouamrane F., Tadjeddine A., Tenne R., Butler J.E., Kalish R., Levy-Clement C., *J Phys Chem*. 102 (1998) 134.
21. Panizza M., Duo I., Michaud P.A., Cerisola G., Comninellis Ch., *Electrochem Solid-State Lett*. 3 (2000) 429.
22. Perret A., Haenni W., Skinner N., Tang X.M., Gandini D., Comninellis Ch., Correa B., Foti G., *Diam Relat Mater*. 8 (1999) 820.
23. El Hajji M., Hallaoui A., Bazzi L., Benlhachemi A., Salghi R., Mansori M., Hilali M., Gavarri J. R., Jbara O., *the 7th National Meeting of Electrochemistry "RNE07"*. (2012) 24.
24. Center of expert testimony in environmental analysis of Quebec, determination of the chemical demand oxygen in the effluents, *MA. 315 DCO 1.0 Rev*. 4 (2006) 12.
25. Mabbott G.A., *An introduction to cyclic voltammetry, J Chem Ed*. 60 (1983) 697.
26. Li M., Feng C.P., Hu W.W., Zhang Z.Y., Sugiura N., *J Hazard Mater*. 162 (2009) 455.
27. Comninellis C., Nerini A.*, J Appl Electrochem*. 25 (1995) 23.
28. Rajkumar D., Palanivelu K., *Electrochemical treatment of industrial wastewater, J Hazard Mater*. 113 (2004) 125.
29. Polcaro A.M., Vacca A., Mascia M., Ferara F., *J Appl Electrochem*. 38 (2008) 979.
30. Hachami F., Salghi R., Mihit M., Bazzi L., Serrano K., Hormatallah A., Hilali M., *International Scientific Journal for Alternative Energy and Ecology*. 62 (2008) 35.
31. Hachami F., Salghi R., Errami M., Bazzi L., Hormatallah A., Chakir A., Hammouti B., *Phys Chem News*. 52 (2010) 106.
32. Comninellis C., Pulgarin C., *J Appl Electrochem*. 21 (1991) 703.
33. Li X.Y., Cui Y.H., Feng Y.J., Xie Z.M., Gu J.D., *Water Res*. 39 (2005) 1972.
34. Li M., Feng C.P., Hu W.W., Zhang Z.Y., Sugiura N., J Hazard Mater. 162 (2009) 455.
35. Belhadj-Tahar N., Savall A., *J Electrochem Soc*. 145 (1998) 3427.
36. Samet Y., Chaabane Elaoud S., Ammar S., *J Hazard Mater*. 138 (2006) 614.
37. Belhadj-Tahar N., Abdelhédi R., Savall A., *J Appl Electrochem*. 39 (2009) 663.
38. Vogt H., Yeager E., Bockris J.O.M., Conway B.E., Sarangapani S., *Comprehensive Treatise of Electrochemistry*. 6 (1983) 459.
39. Balzer R.J., Vogt H., *J Electrochem Soc*. 150 (2003) 11.
40. Tahar N.B. and Savall A., *Journal of Applied Electrochemistry*. 29 (1999) 277.
41. Fleszar B. and Ploszynka J., *Electrochemica Acta*. 30 (1985) 31.
42. Awad Y.M. and Abuzaid N.S., *J Electrochem Soc*. 18 (2000) 227.
43. Wu Z. and Zhou M., *Environmental Science and Technology*. 35 (2001) 2698.

(2015); http://www.jmaterenvironsci.com